Journal of Thermal Analysis and Calorimetry, Vol. 94 (2008) 2, 559–565

THERMAL STABILITY AND FLAME RESISTANCE OF POLYPYRROLE-COATED PET FIBRES

A. Varesano[1], *C. Tonin*[1*], *F. Ferrero*[2] *and Marinella Stringhetta*[3]

[1]CNR-ISMAC, Institute for Macromolecular Studies, C. so G. Pella 16, 13900 Biella, Italy
[2]Politecnico di Torino, Department of Materials Science and Chemical Engineering, C. so Duca degli Abruzzi, 24, 10129 Torino, Italy
[3]ITIS, Laboratorio di Analisi Controllo Qualità, C. so G. Pella 4, 13900 Biella, Italy

Electro-conducting doped polypyrrole was deposited by *in situ* oxidative polymerisation on PET non-wovens. Thermal properties were evaluated by means of DSC and TG in nitrogen and air. Flame resistance tests reveal that coated PET fibres resist to direct contact with fire. By thermal analysis, it was found that PPy reduces the temperature at which thermo-oxidative degradation of PET occurs. Polypyrrole-coated PET non-wovens were heated above the melting point of PET for 30 min. After the heating the fibres become brittle and frail, but SEM observations revealed that they maintained their fibrous shape. A loss of chlorine was found because of intense heating.

Keywords: *flame resistance, PET, polypyrrole, thermal analysis*

Introduction

In situ polymerisation of intrinsically conducting polymers (ICPs) is one of the most promising ways to durably coat textile materials [1] with a conductive, light and flexible thin film. ICPs were applied on wool [2, 3], silk [4], cotton [4], viscose [5], lyocell [5], lycra [6], PET [7–9], nylon [9]. ICPs are doped π-conjugated polymers such as polypyrrole (PPy), polyaniline, polythiophene, polyfuran, poly(*p*-phenylene), poly(phenylenevinylene), poly(3,4-ethylenedioxythiophene) [10]. Generally, ICPs are brittle, insoluble and infusible so chemical and electrochemical coating processes have been developed.

When ICPs are produced by oxidative polymerisation, they contain positive charges on the backbone chain. The mobility of charged species along the polymer chain is responsible for the electrical conduction. The positive charges are stabilized by embedding counter-anions (also called dopants) into the polymer structure.

Along with electrical conductivity, ICPs possess other interesting properties. In particular, due to the high stability of the conjugated structure, they improve the heat resistance of the substrates [4]. The finding that ICPs are flame retardant agents is relatively recent and not yet widely studied and documented.

Usually, thermal stability and flame resistance of polymeric matrixes are enhanced by the addiction of inorganic nanoparticles (e.g. clay) by melt blending [11–13]. Good results were reached when nanoparticles were exfoliated. This requires a thorough study of blending parameters and compatibility, and the whole process is, in some cases, time-expensive [14]. To the best of our knowledge, only PA6-clay nanocomposites were successfully spun into filaments with the aim of producing flame resistance fabrics [15]. On the contrary, the proposed process is simple and relatively cheap, and it has been easily applied to a wide range of textile materials.

In a previous work [16] we observed an increase of about 5°C in the melting point of PPy coated polyethyleneterephthalate (PET) fibres by DSC analysis in inert gas atmosphere. Moreover, SEM observation revealed that the fibres coated with PPy maintained their form even above the melting temperature of PET.

The aim of the present work is to investigate more extensively the thermal stability and flame resistance of PPy coated PET fibres. We suppose that the high thermal stability of char produced at low temperature (just above the PET melting point) in the PPy-PET interface, protects the PET fibres from heat and fire.

Experimental

Materials

The chemicals used were pyrrole, 97% (Py, by Fluka) as monomer, iron(III) chloride hexahydrate, 98% ($FeCl_3 \cdot 6H_2O$, by Fluka) as the oxidant, and 2,6-naphthalenedisulfonic acid, disodium salt, 97%

* Author for correspondence: c.tonin@bi.ismac.cnr.it

1388–6150/$20.00

Akadémiai Kiadó, Budapest, Hungary
Springer, Dordrecht, The Netherlands

(NDS, by Sigma-Aldrich) as dopant. All chemicals were used as received. The substrate was a commercial non-woven 70 mm thick, with a surface density of 300 g m^{-2} composed of 20 μm PET bi-component core-shell fibres.

Methods

The PET non-woven was cut in squares (70×70 mm). PPy deposition was carried out by *in situ* chemical oxidative polymerisation in aqueous solution. The substrates were plunged in 120 mL $FeCl_3$ 0.165 M and NDS 0.015 M (when used) solutions. The monomer was added to a stirred bath reaching the concentration of 0.0745 M; the polymerisation immediately starts and a PPy layer uniformly coats each single fibre. After 4 h, the samples were rinsed in water, squeezed, dried and stored in a conditioned ambient (20°C, 65% R.H.) for at least 24 h before testing. The samples were labelled PPy(FC)/PET when $FeCl_3$ was used and PPy(FC+NDS)/PET when $FeCl_3$ and NDS were used. The PPy deposition increases the mass by 14.4% for the PPy(FC)/PET sample and 28.6% for the PPy(FC+NDS)/PET.

The electrical conductivity of PPy coated PET non-woven was measured in a conditioned laboratory (20°C, 65% R.H.) by means of an electrical circuit consisting of a Metrel potentiometer (0–230 V, 50 Hz), a digital Multimeter Escort 170 and a Supertester 680G ammeter. The resistance values were calculated by the Ohm's law from the current-voltage curves.

Scanning Electron Microscopy (SEM) investigation was performed with a Leica Electron Optics 435 VP with an acceleration voltage of 15 kV, current probe of 400 pA and working distance of 20 mm.

Energy-dispersive X-ray (EDX) spectroscopy was performed by an Oxford Instruments Model 7060 Link ISIS interfaced to a PC using 4096 channels in the range of 10 keV. During EDX analysis, the SEM configuration was 400 pA probe current, 15 kV accelerating voltage and 20 mm working distance.

Before SEM observations and EDX analysis, the samples were mounted on aluminium specimen stubs with double-sided adhesive tape and sputter-coated with silver in rarefied argon (20 Pa) using an Assing® Automatic HR Sputter Coater with a current of 20 mA for 300 s.

Fourier transform infrared (FTIR) spectroscopy was carried out by a Thermo Nicolet Nexus spectrometer by attenuated total reflection (ATR) technique, with the smart endurance accessory in the range from 4000 to 600 cm^{-1}, with 100 scans and 4 cm^{-1} band resolution.

DSC was performed by a Mettler Toledo DSC 821. The calorimeter cell was flushed with 100 mL min^{-1} of nitrogen or air. About 2 mg of sample were used in each test using 40 μL aluminium crucibles. The runs were performed from 30 to 500°C with a heating rate from 5 to 60°C min^{-1}.

TG analysis was performed by a Mettler Toledo TG50 equipped with a TC15 TA Controller. The calorimeter cell was flushed with 100 mL min^{-1} of nitrogen or air. About 3 mg of sample were used in each test using 70 μL aluminium oxide (Al_2O_3) crucibles. The runs were performed from 30 to 500 °C with a heating rate of 20°C min^{-1}.

Flame resistance tests were carried out following the standard test method EN ISO 15025 for limited flame spread of protective clothing against flame and heat. Reproducibility was ensured by testing three specimens for each sample. The specimens were produced by plunging the PET non-woven (with dimensions of 200×160 mm) in 780 mL of the polymerisation bath and treated at the conditions reported above. Each specimen was mounted on a vertical support and subjected to the direct flame contact for 10 s. After that time the flame was moved away from the specimen and the duration of flaming after the first flame application was measured.

Results and discussion

Electrical performances

The electrical performances of PET samples coated with freshly polymerised PPy were measured in a conditioned laboratory (20°C, 65% R.H.). Table 1 reports the resistance values at different voltages calculated by the Ohm's law from the current-voltage curves. The NDS dopant enhances significantly the conductivity, lowering the electrical resistance. The measurements on the PPy(FC+NDS)/PET sample were limited at 20 V to avoid damage of the samples because the temperatures generated by the heating (Joule effect) were too high (up to 70°C). The increase of the sample temperature with increasing the voltage is associated to a resistance decrease [8], being the electrical conduction mechanism of PPy similar to those of semi-conductors.

Table 1 Electrical resistance of PPy(FC)/PET and PPy(FC+NDS)/PET varying the voltage

Voltage/V	Resistance/Ω	
	PPy(FC)/PET	PPy(FC+NDS)/PET
10	178.9	100.6
15	167.8	95.9
20	150.7	90.2
25	144.3	–
30	139.5	–

Moreover, the acidic hydrolysis of $FeCl_3$ produces H^+ ions because of the ionisation of the initial hexa-aquo ferrous complex to form the $[Fe(H_2O)_5OH]^{2+}$ complex [9]. The low pH of the polymerisation bath prevents the nucleophilic attack of water molecules or hydroxyl radicals during the synthesis and enables the formation of extensively conjugated polymer [17].

Surface analysis

During polymerisation, the fibres were coated with an even adherent polymer layer, directly grown on the fibre surface (*in situ*), but the polymer synthesized in the solution bulk formed aggregates of spherical particles [17] weakly linked to the fibre surface [8]. The bulk formation of PPy increased with an increase in the monomer concentration in the polymerisation bath. SEM image reported in Fig. 1a shows the smooth surface of uncoated PET fibre. Figure 1b shows a PPy(FC)/PET fibre coated with an adherent layer of PPy and some aggregates of spherical particles produced in the solution bulk. The sample PPy(FC+NDS)/PET represented in Fig. 1c shows larger amounts of PPy aggregates on the even and adherent PPy layer. The high degree of void of the non-woven structure promotes the formation of globular PPy in solution and the persistence of aggregates on the fibre surface.

The evenness of the coating was assessed using the attenuated total reflection (ATR) technique on FTIR analysis. ATR FTIR is a powerful tool for investigating evenness, thickness and degree of coating because the infrared beam analyses only a thin layer of the fibre surface. Figure 2 shows the typical absorption bands of PET fibres. The sharp and intense peak at 1712 cm^{-1} is attributed to C=O stretching. The broad and strong bands at 1242 and 1095 cm^{-1} are due to C–O and C–O–C stretching, respectively; the sharp peak at 1016 cm^{-1} is associated to C–O–C asymmetric stretching, whereas the C–H bending is responsible for the sharp and strong peak at 723 cm^{-1}. In Fig. 2 is reported the ATR FTIR spectrum of the PPy(FC)/PET characterized by the features of PPy; similar features, not reported here, were obtained for PPy(FC+NDS)/PET samples. The spectrum shows the weak and broad absorption band at 1530 cm^{-1} attributed to the C=C stretching,

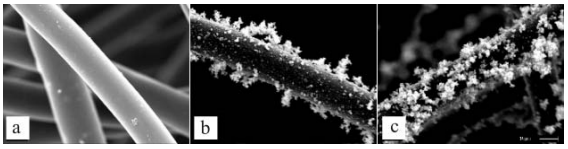

Fig. 1 SEM pictures of a – original PET fibres, b – PPy(FC)/PET and c – PPy(FC+NDS)/PET

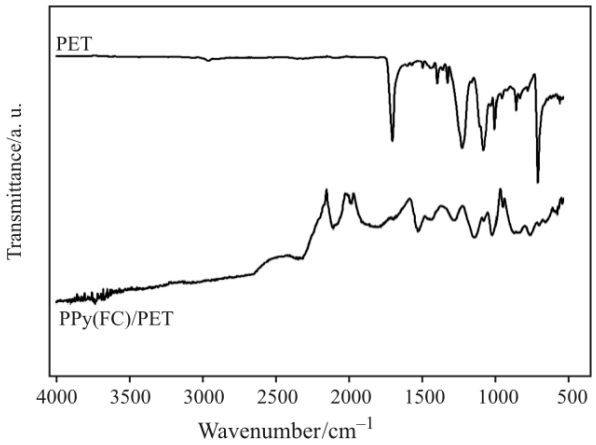

Fig. 2 ATR FTIR spectra of PET and PPy(FC)/PET sample, between 4000 to 500 cm^{-1}

the band at 1450 cm^{-1} assigned to C–C stretching, and the band at 1290 cm^{-1} assigned to C–N vibrations [17, 18]; besides, the peaks at 1150 and 1030 cm^{-1} may be attributed to PPy ring breathing and C–H deformation, respectively [19]. Moreover, in the region between 4000 and 2000 cm^{-1} there is the tail of the electronic absorption band characteristic of conducting PPy [20]. The strong attenuation of the peaks attributed to PET suggests that each fibre is completely coated by a thick (more than 1 μm) PPy layer.

Thermal analysis

The curves of PET, PPy(FC)/PET and PPy(FC+NDS)/PET in nitrogen are reported in Fig. 3a. PET fibres show a glass transition at about 72°C (associated with an endothermic event due to tempering during the industrial production process) and two melting temperatures at 246.8 and 251.5°C related to the melting of fibre shell and core respectively, followed by degradation. The curve of PPy coated PET samples shows a shift of these melting points to higher temperatures, namely 252.2 and 260.2°C.

The thermal mass loss traces obtained with the TG analysis from PET, PPy(FC)/PET and PPy(FC+NDS)/PET are reported in Fig. 3b. The PPy coated fibres show an initial mass loss greater than those of PET due to the loss of humidity and chlorine [21] (also see EDX analysis below). In particular, the PPy(FC+NDS)/PET shows a mass loss of about 4% in the temperature range from 50 to 110°C, probably due to humidity evaporation. The onset of thermal degradation of PET sample occurs at about 370°C, whereas PPy(FC)/PET and PPy(FC+NDS)/PET start degrading at lower temperatures, about 350 and 340°C, respectively. It was pointed out by Wu *et al.* [6] that PPy coated fibres are less stable to heating than uncoated fibres because of the breakdown of the polypyrrole backbone, but it is also possible that PPy

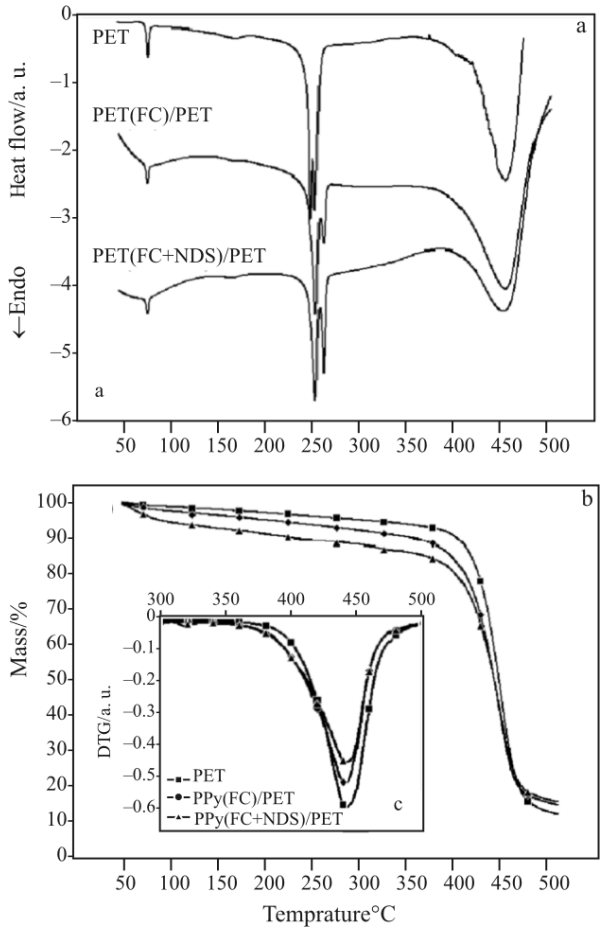

Fig. 3 a – DSC and b – TG results of PET, PPy(FC)/PET sample and PPy(FC+NDS)/PET sample, from 30 to 500°C with 20°C min^{-1} heating rate in nitrogen. c – DTG curves are reported in the box from 300 to 500°C

coated fibres, maintaining the fibrous form (see SEM analysis below), expose to degradation a greater surface compared with pure PET which forms a drop when it melts.

The mass of the residual char at 500°C was higher in the coated sample (12.6% for PET, 15.3% for PPy(FC)/PET and 16.1% for PPy(FC+NDS)/PET). Therefore, the undegradable fractions of the PPy(FC)/PET and PPy(FC+NDS)/PET samples measured at 500°C were about 20% higher than the untreated PET.

Table 2 reports data about DSC and TG traces shown in Fig. 3. PPy(FC)/PET and PPy(FC+NDS)/PET have lower melting enthalpies than pure PET because PPy does not melt. The smaller mass loss associated to degradation of the treated samples is due to the presence of PPy that, at high temperature, produces more stable char than PET. These findings are in good agreement with recent literature. In particular, Cataldo and Omastová reported that PPy produced with $FeCl_3$ as oxidant has a quite good thermal stability, in fact its total mass loss is 15% at about 515°C and only 30% at 900°C [22].

DSC runs were carried out at different heating rates to confirm the shift of the melting points and ensure that this finding was not a delay due to an insufficient contact between sample and crucible during the analysis. As reported in Table 3, the PET melting points of PPy coated PET fibres were independent by the heating rate. The first melting temperature is ~251°C and the second is ~259°C in all the runs. Also the melting enthalpy was practically constant (average value 33.3 J g^{-1}).

The curves of PET and PPy(FC)/PET in air flow are reported in Fig. 4a. The glass transition of PET occurs at about 72°C. The PET sample shows the two melting temperatures at 246.6 and 251.6°C, followed by thermo-oxidative degradation at about 430°C. The curve of PPy coated PET sample shows an evident melting point at 252.2°C, followed by two exothermic events. The first starts immediately after the melting. The flammability of polymers is related to their thermo-oxidative degradation at high temperatures when the polymer is subjected to sufficient heat flux. Flame-retardants may act by altering the pathway of the pyrolytic decomposition of the polymer or by scavenging carrier species, which are required during the oxidation of volatile products in the flame [22]. It seems that PPy acts as a flame retardant agent by reducing the temperature at which thermal oxidation of PET occurs producing char.

The thermo-oxidative mass loss traces obtained with the TG analysis from pure PET and PPy(FC)/PET are reported in Fig. 4b. PET degrades in the range 350–470°C with a mass loss of 83.0%. The thermal oxidative decomposition of

Table 2 DSC and TG analysis on PET, PPy(FC)/PET and PPy(FC+NDS)/PET at 20°C min^{-1} in nitrogen

Sample	PET	PPy(FC)/PET	PPy(FC+NDS)/PET
Glass transition/°C	72.3	72.9	73.0
First melting temperature/°C	246.8	252.2	252.5
Second melting temperature/°C	251.5	260.2	260.8
Total melting enthalpy/J g^{-1}	–36.4	–33.0	–28.4
Onset degradation/°C	370	350	340
Mass loss during degradation /%	78.8	70.6	68.7

Table 3 DSC analysis on PPy(FC)/PET at increasing heating rates in nitrogen

Heating rate/°C min^{-1}	5	10	20	30	60
First melting temperature/°C	251.1	251.6	252.2	251.8	251.7
Second melting temperature/°C	258.5	258.8	260.2	260.9	260.9[a]
Total melting enthalpy/J g^{-1}	–32.0	–33.8	–33.0	–33.9	–33.9

[a]Visible as shoulder

PPy(FC)/PET starts degrading in two steps with a total mass loss of 75.3%.

Analysis after heating

PPy coated PET non-wovens were placed in an oven at 280°C (above the melting points of PET and near the exothermic decomposition temperature, see Fig. 4) for 30 min in air. As shown in the pictures of Fig. 5, after the thermal treatment the PPy coated PET non-wovens (Fig. 5b) still kept their form, while uncoated PET melted (Fig. 5a). However, the PPy coated PET fibres became rather brittle. This is consistent with the reduction of the thermal oxidation temperature of PET. Moreover, SEM analysis on samples after high temperature treatments showed that all the fibres coated with PPy kept their fibrous shape, only the surface morphology changed. As Figs 6a and b show, the aggregates on the fibre surface have lost the spherical structure and appear incorporated in the fibres.

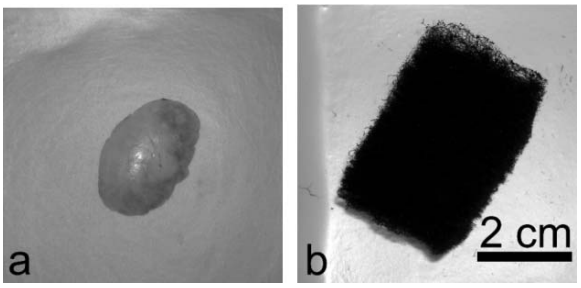

Fig. 5 Pictures of a – molten PET non-woven and b – PPy(FC)/PET after thermal treatment at 280°C for 30 min at air

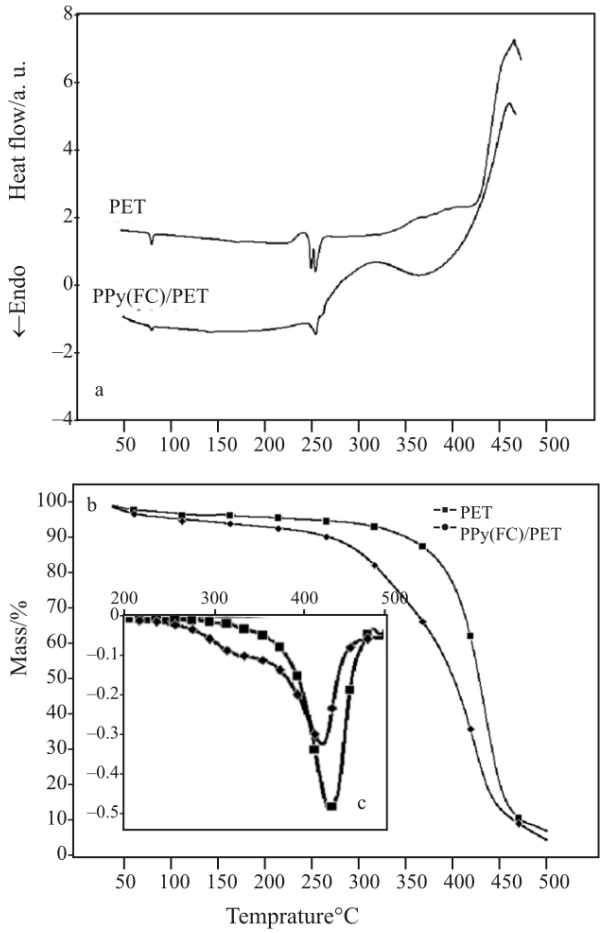

Fig. 4 a – DSC and b – TG results of PET and PPy(FC)/PET sample, from 30 to 500°C with 20°C min^{-1} heating rate in air. c – DTG curves are reported in the box from 200 to 500°C

Energy-dispersive X-ray (EDX) spectroscopy results are reported in Fig. 7. The samples were sputter-coated with silver (Ag L 3.02 and 3.17 keV) to achieve an acquisition rate more than 500 cps. EDX analysis shows that both PPy(FC)/PET and PPy(FC+NDS)/PET freshly polymerised contained significant amount of chlorine (signal at 2.62 keV attributed to Cl Kα). It is well known that Cl^- ions from $FeCl_3$ are embedded in the PPy matrix as counter-ions during polymerisation [1, 2, 21, 22]. The signal at 2.27 keV in the spectrum of the PPy(FC+NDS)/PET sample is attributed to sulphur (S Kα) of the NDS embedded in PPy as counter-ion. The EDX spectra also show peaks due to carbon (C Kα 0.27 keV), oxygen (O Kα 0.53 keV) belonging to PET or NDS, and nitrogen (N Kα 0.39 keV)

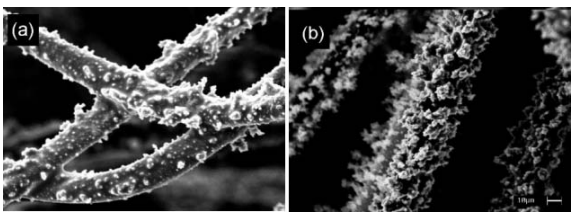

Fig. 6 SEM pictures of a – PPy(FC)/PET and b – PPy(FC+NDS)/PET after thermal treatment at 280°C for 30 min at air

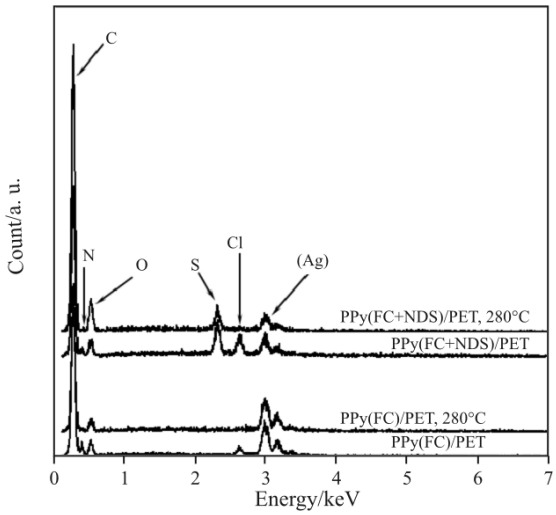

Fig. 7 EDX spectra of PPy(FC)/PET before and after thermal treatment, and PPy(FC+NDS)/PET before and after thermal treatment

belonging to PPy. Iron peaks (Fe K 6.3 keV, Fe L 0.7 keV), as a residue of oxidative polymerisation, were not found in the spectra. The nitrogen signal is present in all the EDX spectra, also after thermal treatments at 280°C in air. The peak from chlorine disappears in spectra of samples submitted to thermal treatments. It is supposed that chloride anions and hydrogen of the polymer chains react at high temperature to form volatile HCl. Moreover, Carrasco *et al.* [21] found that there is a release of HCl from the PPy due to heating. It is worth noting that the peak associated to sulphur is still present after thermal treatment.

Figure 8 shows FTIR spectra of thermal-treated samples PPy(FC)/PET and PPy(FC+NDS)/PET compared to pristine PET. The spectra of thermal-treated samples showed the features of PET excepting for the tail of the electronic absorption band in the region between 4000 and 2000 cm^{-1} attributable to PPy. The weakness of this signal indicates a low electrical activity.

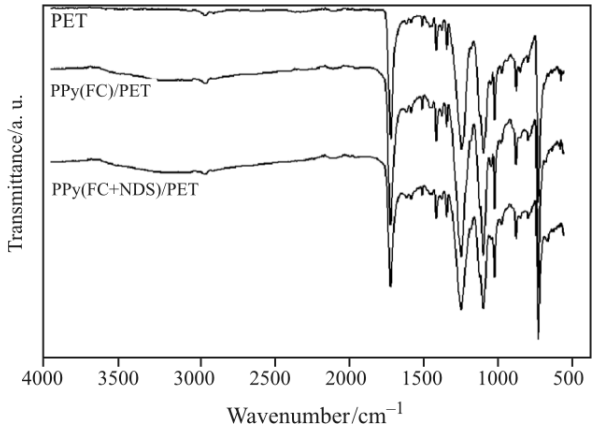

Fig. 8 ATR FTIR spectra of PET, PPy(FC)/PET sample and PPy(FC+NDS)/PET, between 4000 to 500 cm^{-1}, after thermal treatment at 280°C for 30 min at air

Flame resistance

Specimens of PET, PPy(FC)/PET and PPy(FC+NDS)/PET were subjected to direct flame following the standard test method EN ISO 15025. The pictures in Fig. 9 illustrate the tests.

The untreated PET non-woven immediately melted in drops on contact with flame and a hole was produced on the sample in about 2 s, thus untreated PET did not pass the test.

Both the treated samples (PPy(FC)/PET and PPy(FC+NDS)/PET) resisted to direct contact with fire without significant changes in their aspect. The flame persisted on the samples after the flame contact for 1.9 and 1.1 s, respectively (the times are the average values obtained from three tests). The flame was weak and self-extinguishing. No hole was produced on the surface: flame and heat did not pass through the sample. No drop of molten polymer was observed.

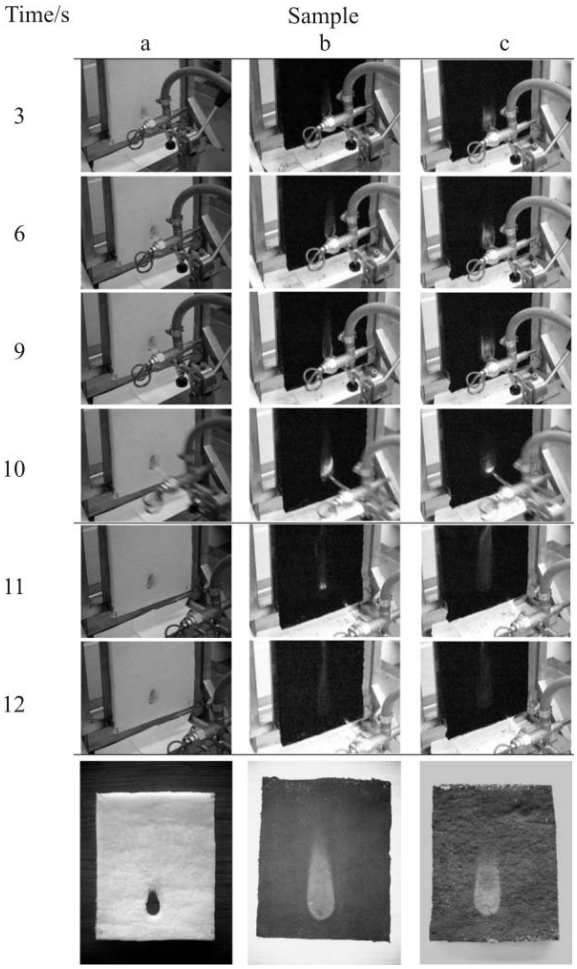

Fig. 9 Pictures of the flammability tests of a – untreated PET non-woven, b – PPy(FC)/PET and c – PPy(FC+NDS)/PET. The first column reports the timing. After 10 s the flame was moved away from the specimens. The pictures in the bottom line illustrate the specimens after the tests

Conclusions

Electro-conducting polypyrrole deposited by *in situ* chemical oxidation on PET non-wovens in chloride and chloride-NDS doped forms. Coating evenness was evaluated by ATR FTIR. PPy coated PET non-woven shows interesting properties of heat and flame resistance. The shift (5°C higher) of melting points of PET on coated samples was confirmed by DSC runs with different heating rates. Coated samples maintain their fibrous form also when placed in an oven at 280°C for 30 min in air and after thermal analysis up to 500°C. SEM observation revealed that the fibres coated with PPy maintained their form even above the melting temperature of PET and after polymer degradation. We supposed that the high stability of wrapping PPy protects the PET fibres. EDX analyses reveal a loss of chlorine embedded in the PPy matrix as counter-ions as the temperature rises (it is supposed that HCl is formed at high temperature) while sulphur of NDS embedded in PPy is more stable. Moreover, PPy coated PET fibres resist to the direct contact with flames and pass the standard test method EN ISO 15025. PPy gives good flame-proof property to PET because of its good chemical stability, and because it lowers the oxidative decomposition temperature of PET as revealed by TG analysis.

References

1 A. Malinauskas, Polymer, 42 (2001) 3957.
2 A. Varesano, L. Dall'Acqua and C. Tonin, Polym. Degrad. Stab., 89 (2005) 125.
3 R. C. Foitzik, A. Kaynak, J. Beckmann and F. M. Pfeffer, Synth. Met., 155 (2005) 185.
4 S. H. Hosseini and A. Pairovi, Iranian Polym. J., 14 (2005) 934.
5 L. Dall'Acqua, C. Tonin, R. Peila, F. Ferrero and M. Catellani, Synth. Met., 146 (2004) 213.
6 J. Wu, D. Zhou, C. O. Too and G. G. Wallace, Synth. Met., 155 (2005) 698.
7 B. Kim, V. Koncar, E. Devaux, C. Dufour and P. Viallier, Synth. Met., 146 (2004) 167.
8 E. Hakansson, A. Kaynak, T. Lin, S. Nahavandi, T. Jones and E. Hub, Synth. Met., 144 (2004) 21.
9 R. V. Gregory, W. C. Kimbrell and H. H. Kuhn, Synth. Met., 28 (1989) 823.
10 A. G. MacDiarmid, Angew. Chem., Int. Ed., 40 (2001) 2581.
11 R. Peila, S. Lengvinaite, G. Malucelli, A. Priola and S. Ronchetti, J. Therm. Anal. Cal., 91 (2008) 107.
12 S. P. S. Ribeiro, L. R. M. Estevão and R. S. V. Nascimento, J. Therm. Anal. Cal., 87 (2007) 661.
13 E. M. Araújo, R. Barbosa, A. D. Oliveira, C. R. S. Morais, T. J. A. deMélo and A. G. Souza, J. Therm. Anal. Cal., 87 (2007) 811.
14 A. R. Horrocks, B. K. Kandola, P. J. Davies, S. Zhang and S. A. Padbury, Polym. Degrad. Stab., 88 (2005) 3.
15 S. Bourbigot, E. Devaux, X. Flambard, Polym. Degrad Stab., 75 (2002) 397.
16 A. Varesano, A. Ibarzabal Ferrer and C. Tonin, e-Polymers, 022 (2007).
17 H. V. Rasika Dias, M. Fianchini and R. M. Gamini Rajapakse, Polymer, 47 (2006) 7349.
18 H. Shiigi, M. Kishimoto, H. Yakabe, B. Deore and T. Nagaoka, Anal. Sci., 18 (2002) 41.
19 R. G. Davidson and T. G. Turner, Synth. Met., 72 (1995) 121.
20 N. Toshima and O. Ihata, Synth. Met., 79 (1996) 165.
21 P. M. Carrasco, M. Cortazar, E. Ochoteco, E. Calahorra and J.A. Pomposo, Surf. Interface Anal., 39 (2006) 26.
22 F. Cataldo and M. Omastová, Polym. Degrad. Stab., 82 (2003) 487.

Received: November 13, 2007
Accepted: April 16, 2008
OnlineFirst: August 15, 2008

DOI: 10.1007/s10973-007-8639-x